International Journal of Industrial Ergonomics 41 (2011) 437–446

Contents lists available at ScienceDirect

International Journal of Industrial Ergonomics

journal homepage: www.elsevier.com/locate/ergon

An EMG-based model to estimate lumbar muscle forces and spinal loads during complex, high-effort tasks: Development and application to residential construction using prefabricated walls

Bochen Jia [a], Sunwook Kim [a], Maury A. Nussbaum [a,b,*]

[a] Department of Industrial and Systems Engineering, Virginia Tech, Blacksburg, VA 24061, USA
[b] School of Biomedical Engineering and Science, Virginia Tech, Blacksburg, VA 24061, USA

ARTICLE INFO

Article history:
Received 22 February 2010
Received in revised form
24 February 2011
Accepted 29 March 2011
Available online 6 May 2011

Keywords:
Spine
Model
Residential construction
EMG
Prevention-through-design

ABSTRACT

Residential building construction is moving toward more industrialized construction methods (e.g., use of prefabricated wall or "panels"), yet remains one of highest risk sectors for work-related musculoskeletal disorders. The centralized design process inherent in the use of wall panels offers the potential for proactive control of musculoskeletal risks, consistent with the prevention-through-design (or PtD) philosophy. As part of an ongoing effort to incorporate ergonomics into panel design, estimates of low back loading and injury risk were needed over a range of tasks performed during panelized construction. Here, a free-dynamic, three-dimensional, electromyography-based model was developed to provide such estimates, which was a modification of an earlier, relatively coarser model. Specific modifications included a more detailed representation of lumbar muscle anatomy and contraction dynamics, high-pass filtering of electromyograms to better represent muscle activation levels, and an enhanced calibration procedure through which five model parameters are specified on an individual basis and used to estimate lumbar muscle forces. With these enhancements, the predictive ability of the model was assessed over a wide range of simulated panel erection tasks. Predicted model parameters corresponded well with values reported earlier. Reasonable levels of correspondence were found between measured and predicted lumbosacral moments, though predictive ability varied between tasks and rotation planes.
Relevance to industry: Wall panels are representative of the current trend toward increasing use of industrialized methods in residential construction. Model-based estimates can be used as part of a larger project to facilitate proactive design of residential construction using panelized walls in order to reduce musculoskeletal exposures and spine injury risks.

1. Introduction

Work-related injuries and illnesses pose a continuing threat to the health and well-being of U.S. construction workers and to the productivity of construction firms. Our emphasis here is on residential construction, a large economic activity requiring over 1 million workers in 2006 (Mullins, 2006), and which is projected to grow by ~20% in the approaching decade (BLS, 2008c). Residential construction has been recognized as among those sectors having a relatively high prevalence of work-related injuries and illnesses (BLS, 2008a,b; Schoonover et al., 2010), with injury rates likely higher than those reported in centralized databases (Lipscomb et al., 2003a). In this sector, overexertion injuries are the 2nd largest source of direct costs, and more than half of these injuries result from postural and unexpected loads (Lipscomb et al., 2003a,b). Modern residential construction can be viewed as a craft-based enterprise driven by a centralized design process, but this design is detached from the actual construction process on site (e.g., method of assembly) and often takes little or no account of the ergonomic impacts on workers (Wakefield et al., 2001; O'Brien and Beliveau, 2002). Modern construction, and to some extent residential construction, is also moving toward increasing prefabrication, one example of which is the use of panels (panelized walls) that are increasingly being adopted by residential U.S. production builders (Wakefield et al., 2001).

Panels are designed by a central designer based on several criteria (e.g., preferred and maximal lengths), are built in a manufacturing facility, and are then erected by workers on site.

* Corresponding author. Department of Industrial and Systems Engineering, Virginia Tech, 250 Durham Hall (0118), Blacksburg, VA 24061, USA. Tel.: +1 540 231 6053; fax: +1 540 231 3322.
E-mail address: nussbaum@vt.edu (M.A. Nussbaum).

0169-8141/$ – see front matter © 2011 Elsevier B.V. All rights reserved.
doi:10.1016/j.ergon.2011.03.004

Nomenclature

CW	clockwise
CCW	counter clockwise
DSS	decision support system
EF, k_1	EMG-to-force relationship
EMG	electromyography
nEMG	normalized EMG
EO	external oblique
FL	force–length relationship
FP, k_2	muscle passive components
FV	force–velocity relationship
GTD, k_3	global time delay
IO	internal oblique
L_i	length of ith muscle
LBP	low back pain
ILL	iliocostalis lumborum pars lumborum
ILT	iliocostalis lumborum pars thoracis
LTL	longissimus thoracis pars lumborum
LTT	longissimus thoracis pars thoracis
MF	multifidus
MVC	maximum voluntary contraction
PCSA	physiological cross-sectional area
RA	rectus abdominis
S_F&S_E	muscle stress for flexor and extensor
WMSD	work-related musculoskeletal disorders

This centralized design process yields an opportunity to control the risk of work-related musculoskeletal disorders (WMSDs) early in the project lifecycle, specifically at the design phase. Such an approach is considered to be the most effective way of preventing and controlling occupational injuries and illnesses, and is consistent with the prevention-through-design (PtD) philosophy (Schulte et al., 2008). PtD has been promoted by a number of investigators and practitioners, and has begun to gain support and/or interest from involved stakeholders (e.g., Hinze and Wiegand, 1992; Hecker et al., 2004; Schulte et al., 2008).

Our group has endeavored to implement a PtD approach to panelized construction by developing a decision support system (DSS) that enables panel designers to enhance both ergonomics and productivity at the design phase (Nussbaum et al., 2009). This is a software-based approach, involving a simulation of the discrete tasks involved with panelized construction. Underlying this is a need to estimate the ergonomic consequences of a given design, one important aspect of which are the physical demands and risks at the lumbar spine. For all work-related injuries, the trunk is among the most commonly injured body parts, accounting for 32% of total nonfatal occupational injuries and illnesses in construction (BLS, 2008a), and this motivated the current focus on biomechanical modeling of the low back. Further, a preliminary evaluation using the NIOSH lifting equation (Waters et al., 1994) indicated that wall erection tasks impose substantial risk of low back injury (lifting indexes rarely <1 and often >3). To make the DSS broader and more representative in terms of estimating the influence of alternative design approaches, more refined estimates of low back loading and injury risk are required. Yet, to the authors' knowledge, no previous evidence of such outcomes is available for the broad range of existing panel erection tasks.

Musculoskeletal modeling is an appealing approach to determine the complex internal loads on the lumbar spine borne by the muscles, joints, and soft tissue during diverse work tasks, since there is lack of non-invasive methods to measure *in vivo* muscle forces and internal spinal loads accurately. Over the past several decades, a variety of biomechanical models have been developed to predict internal loads on the lumbar spine. Most contemporary approaches involve multiple muscles, since earlier models (e.g., single-equivalent muscle) do not account for the effects of muscle co-activation. Diverse strategies have been used in multiple muscle models to partition loads among the several muscles included. These strategies include those based on optimization (e.g., van Dieën, 1997), neural networks (e.g., Nussbaum and Chaffin, 1996), stochastic models (e.g., Mirka and Marras, 1993), electromyography (EMG) (e.g., McGill and Norman, 1986; Granata and Marras, 1995; Nussbaum and Chaffin, 1998), and EMG-optimization hybrids (e.g., Cholewicki and McGill, 1994). Excepting those approaches based on EMG, models using the alternative methods typically do not account for either inter- or intra-individual differences in muscle recruitment strategies.

In contrast, EMG-based models inherently account for different recruitment strategies, including diverse levels of muscle cocontraction, both within and across individuals. Several research groups (McGill and Norman, 1986; Granata and Marras, 1993, 1995; van Dieën and Kingma, 2005) have developed EMG-based spine models, each of which differs in terms of model complexity, underlying approaches and/or assumptions. Regarding the latter, some approaches have included model parameters that improve performance yet have unclear physiological interpretations or are not specific to individuals. Earlier, we developed a dynamic EMG-based model based on participant-invariant parameters that were specified through a calibration procedure (Nussbaum and Chaffin, 1998). This model, however, included only coarse representations of muscles and was evaluated only for a relatively narrow range of dynamic tasks.

The objective of this study was to extend our original model by incorporating more detailed and complete muscle anatomy, muscular dynamics, and a refined modeling process, to predict trunk muscle forces and low back loads during a wide range of panel erection tasks (such tasks are inherently complex and dynamic). In this paper, the model development process is comprehensively described, and model performance was evaluated using a wide range of panel erection tasks simulated in a laboratory environment.

2. Methods

2.1. Model development

A three-dimensional, dynamic model of the lumbar spine was developed, incorporating detailed musculature representations, muscle kinematics, and muscle activation dynamics. Surface EMG, trunk kinematics, and individual anthropometry are inputs to the model, which consists of three components: 1) an anatomical model representing muscle geometry and kinematics, 2) an EMG-based muscle model describing muscle force dynamics, and 3) a spine stiffness model quantifying the effects of motion segment passive tissues. When implementing the model, a set of participant-invariant model parameters is obtained from calibration procedures. In the following, each component is described, as well as methods used for calibration and an experiment from which data were obtained to evaluate model performance.

2.2. Anatomical model

Participant-specific muscle geometry and trunk kinematic were obtained using the AnyBody™ musculoskeletal modeling system (v3.0, repository 7, AnyBody Technology, Aalborg, Denmark). The muscular representation included 16 muscles crossing the lower

lumbar region, divided into a group of flexors[internal oblique (IO), external oblique (EO), rectus abdominis (RA)] and a group of extensors [iliocostalis lumborum pars lumborum (ILL), iliocostalis lumborum pars thoracis (ILT), multifidus (MF), longissimus thoracis pars lumborum (LTL), and longissimus thoracis pars thoracis (LTT)]. Deeper torso muscles (e.g., psoas, quadratus lumborum and transverse abdominis) were not included, due to their relatively small contribution to lumbar kinetics (McGill, 1992) and the difficulty in detecting their activity using surface EMG during highly dynamic tasks, although McGill et al. (1996) showed that such activity can be predicted during a limited set of task types.

Each of the represented muscles was sub-divided into multiple functional fascicles, with distinct insertions and origins, replicating the diverse anatomy within each muscle. Thereby, 92 fascicles were included in the anatomical model (MF = 24, ILL = 8, ILT = 16, LTL = 10, LTT = 14, EO = 4, IO = 12, RA = 4). As in earlier work (McGill and Norman, 1986; Bogduk et al., 1992; Cholewicki et al., 1995; van Dieën and Kingma, 2005), fascicles within each muscle were assumed to have equal activation levels. Initial insertions, via points, and origins were defined according to existing evidence (de Zee et al., 2007), and were scaled based on individual stature and body mass (AnyBody, v3.0). Measured trunk kinematics (described in Section 2.7) were input to the anatomic model, yielding estimates of the line-of-action, length, and velocity at each sample instant.

2.3. EMG-based muscle model

The current model is a refinement of that described by Nussbaum and Chaffin (1998) and was implemented in MATLAB™ (v7.2, The MathWorks Inc., Natick, MA, USA). In this approach, the force, $F_i(t)$, generated by the ith muscle fascicle at a given time t, was determined on an individual basis and as a function of: normalized EMG (*nEMG*); EMG-to-force relationship (EF; parameter k_1); muscle stress (maximal force per unit area) for flexors (S_F) and extensors (S_E); physiological cross-sectional area (PCSA); muscle passive contribution (FP; k_2); and functional properties [time lag between EMG and measured force (k_3), force–length (FL), and force–velocity (FV) relationships]. As such, a unique model is obtained for each individual, by specifying the five noted parameters during calibration (described in Section 2.6):

$$F_i(t) = F_{\max_i} \times \left[\mathrm{EF}\left(\mathrm{nEMG}_i(t, k_{3,i}), k_{1,i}\right) \times \mathrm{FL}(L_i) \times \mathrm{FV}(V_i) + \mathrm{FP}(L_i, k_{2,i})\right] \quad (1)$$

where $F_{\max_i}$ represents muscle strength (i.e., the product of muscle stress and PCSA). L_i represents the length of ith muscle. PCSAs were initialized using values from the literature (Stokes and Gardner-Morse, 1999), and the contribution of PCSA to individual differences in muscle strength was incorporated through specification of S_F and S_E during calibration.

Several modifications to the earlier approach were made: 1) to refine and improve the representation of muscle geometry (as noted above) and functional properties, 2) to specify more efficiently some of the parameters, and 3) to allow the model to be used in more complex, dynamic, and high-effort tasks. The influence of muscle contraction velocity on force generation capability was represented using the FV relationship reported by McGill and Norman (1986):

$$\begin{aligned} \mathrm{FV}(V_i) &= (0.9 + 0.25V_i)/(V_i + 0.9) \quad \text{for } V_i < 0 \text{ (concentric)} \\ \mathrm{FV}(V_i) &= 1 + 1.6V_i \quad \text{for } 0 \le V_i < 0.125 \\ &\quad \text{(isometric to slow eccentric)} \\ \mathrm{FV}(V_i) &= 1.2 \quad \text{for } V_i \ge 0.125 \text{ (fast eccentric)} \end{aligned} \quad (2)$$

where FV is a scaling factor accounting for the influence of contraction velocity V_i (m/s) of the ith muscle fascicle on force generation capacity.

The time lag between the onset of EMG and the onset of force production, often referred to as electromechanical delay (EMD), is an important parameter in modeling skeletal muscles (Cavanagh and Komi, 1979; Norman and Komi, 1979). Determination of a muscle-specific EMD, however, is difficult since individual muscles can be rarely isolated; instead, they work together as synergists or antagonists (Ross et al., 1993; Thelen et al., 1995; van Dieën et al., 2003a). In biomechanical modeling, estimates of electromechanical delay (EMD) are usually made by assuming that only measured agonistic muscles are active, and with minimal (or no) antagonistic cocontraction (e.g., Vos et al., 1990). Here, a new approach was used, the global time delay (GTD), which accounts for individual recruitment strategies. Given that substantial antagonist and agonist activity was present, this approach was expected to provide an improved estimate of EMD. Measured moments were obtained via inverse dynamics from AnyBody™. Predicted moments were not available at this point (i.e., the EMG-based model was not yet fully specified), and so were indirectly estimated. As such, a weighted summation of nEMG, $[\sum(w_i \times \mathrm{nEMG}_i)]$, was used to estimate the total moment contribution of muscles spanning the L5/S1 joint; this estimate is proportional to the predicted moment. Muscle contraction patterns were determined from nEMG and the weighting factors (w_i), representing the maximum moment contribution of each muscle fascicle to the net moment, were calculated as the ratio of maximum contributions of the ith fascicle relative to the total contribution across all muscles:

$$w_i = \mathrm{EMG}_{\max,i}(r_i \times f_i) / \sum_i \mathrm{EMG}_{\max,i}(r_i \times f_i) \quad (3)$$

where r_i is the position vector of the ith fascicle relative to the L5/S1 rotation center and f_i is a unit vector along the fascicle's line-of-action.

GTD was determined as the time offset that maximized the correspondence (r^2) between measured and predicted triaxial moments at L5/S1 during model calibration (described in Section 2.6). The average estimated GTD across several maximal efforts was incorporated into the EMG-to-force relationship (as parameter k_3) to account for the time lag between measured force and global muscle activation. Note that the above procedure assumed a linear relationship between EMG and muscular force, which is consistent with earlier evidence (Nussbaum and Chaffin, 1998; Theado et al., 2007; Brown and McGill, 2008) and our subsequent calibration results. Though a linear EMG–force relationship is recommended to account for muscle cocontraction (Brown and McGill, 2008), further work is needed to allow for potential nonlinearities in the force–EMG relationship during such calibration (as was assumed here), and to account for EMD differences between individual muscles and/or fascicles as well the influence of contraction velocity, initial muscle length, and fiber type composition (Viitasalo and Komi, 1975; Cavanagh and Komi, 1979; Vink et al., 1989; van Dieën et al., 1991).

2.4. Spine stiffness model

Forces and moments generated by deformation of passive spine elements at L5/S1 were estimated from existing literature. Spine stiffness was obtained from the motion segment stiffness matrix (Panjabi et al., 1977), with consideration of axial compressive preloads (Stokes and Gardner-Morse, 2003; Gardner-Morse and Stokes, 2004). The spine stiffness contribution (F_{stiff}) at the L5/S1 joint in three orthogonal axes (x, y, z) is expressed as:

$$F_{\text{stiff}}(t) = \begin{bmatrix} \gamma_x(t) \\ \gamma_y(t) \\ \gamma_z(t) \\ \mu_x(t) \\ \mu_y(t) \\ \mu_z(t) \end{bmatrix} = \begin{bmatrix} \ddots & & \\ & \left(c_2\left(1-e^{c_1 F}\right)+K_0\right) & \\ & & \ddots \end{bmatrix}_{6\times 6} \begin{bmatrix} \delta_x(t) \\ \delta_y(t) \\ \delta_z(t) \\ \theta_x(t) \\ \theta_y(t) \\ \theta_z(t) \end{bmatrix} \tag{4}$$

where coefficients c_1, c_2 and the non-preload stiffness K_0 were obtained based on Stokes and Gardner-Morse (2003). F is the axial compressive preload from upper body weight, estimated based on segment mass-center locations and mass distributions as summarized in Chaffin et al. (2006, pp. 37–49). The terms $\delta(t)$ and $\theta(t)$ are the relative intervertebral translation and rotation, respectively, about the L5/S1 joint, and were calculated based on trunk kinematics. Finally, γ and μ respectively represent force and moment generated at L5/S1 by deformation of passive spine elements (i.e., disc, ligaments, facets).

2.5. Spine force and moment prediction

Internal (reactive) spinal forces generated by muscles at the L5/S1 joint (e.g., compression and shear forces) were determined from the vector sum of estimated muscle forces (Granata et al., 1999; van Dieën and Kingma, 1999). Internal spinal moments, $M(t)$, produced by the 92 muscle fascicles $[r_i \times F_i(t)]$ and deformation of passive spine elements (μ) were then obtained as:

$$M(t) = \sum_{i}^{92} r_i \times F_i(t) + \mu(t) \tag{5}$$

2.6. EMG data collection and model calibration

The bilateral activity of three flexors (IO, EO and RA) and four extensors (MF, ILL, LTL and LTT) was monitored using two telemetered EMG systems (TeleMyo 900, Noraxon, AZ). Pairs of disposable bipolar Ag/AgCl electrodes (AccuSensor, Lynn Medical, MI) with a 2.5 cm inter-electrode distance were placed bilaterally on the skin surface as described by van Dieën (1997) and Potvin et al. (1996). A single pair of electrodes was used to monitor the LTL and ILT on each side (Cholewicki and McGill, 1996; van Dieën, 1996, 1997; Kiefer et al., 1998; Danneels et al., 2001b; Coorevits et al., 2005). This approach was based on previous evidences that ILT and LTL are synergistic and contain similar fiber type distributions (Thorstensson and Carlson, 1987), and prior strategies used to monitor the activations of those muscles (Vink et al., 1987; Danneels et al., 2001a; van Dieën et al., 2003b). Skin preparation involved abrasion and cleaning with a mild alcohol solution, and inter-electrode impedance was verified as <10 kΩ.

Raw EMG signals were collected at 1080 Hz, band-pass filtered (20–400 Hz), and subsequently processed using the following steps. First, raw EMG was high-pass filtered using a cut-off frequency of 300 Hz (bidirectional 1st-order Butterworth). High-pass filtering was used as it has shown improvements in the representation of muscle activations (Potvin and Brown, 2004; Staudenmann et al., 2007; Keenan and Valero-Cuevas, 2008; Brown et al., 2009). Second, the high-pass filtered EMG signals were rectified. Third, the rectified EMG signals were low-pass filtered at 2 Hz (bidirectional 1st-order Butterworth) to create a smoothed curve more closely matching actual force output (Potvin and Brown, 2004; Staudenmann et al., 2007). Finally, the processed EMG signals were normalized using individual maximal and minimal values (Mirka, 1991). The former were obtained from maximum voluntary contractions (MVCs) as described below, while minimal values were obtained for the ventral and dorsal muscles in relaxed supine and prone positions, respectively.

Model parameters were specified for each participant, using a set of MVCs and a maximum passive trunk flexion task (*cf.* Nussbaum and Chaffin, 1998). MVCs comprised a set of ramp-up, hold, and ramp-down efforts, during which the participant stood in a custom frame attached to a force platform (Bertec 4550-08, Worthington, OH). Therein, the pelvis and lower legs were securely but comfortably restrained by pelvic, thigh, and knee straps. Participants performed three trials, with one minute of rest between MVCs, for each of six efforts: trunk flexion/extension, right/left lateral bending, and clockwise/counterclockwise axial rotation. Excepting trunk extension, which was done in 20° of trunk flexion, all other efforts were in the upright posture. For the passive flexion task, participants stood on a force platform (AMTI OR6-7-1000, Watertown, MA) with their feet together in fully flexed posture while holding a 6.5 kg mass in their hands, and were instructed to relax their trunk muscles.

Muscle stresses for flexors and extensors (S_F and S_E) and k_1 were determined as a group, using data from the MVCs, through an iterative procedure that minimized lumbar moment differences (measured vs. predicted) in all three rotation planes. Similarly, muscle passive stiffness (k_2) was identified as the value that minimized moment prediction differences during the passive flexion task. All model parameters were established prior to evaluation trials (as described in Section 2.7) and were held constant thereafter.

2.7. Model evaluation

The spine model was evaluated using data obtained from an experiment involving simulated residential construction using panelized walls, as part of a larger investigation (Nussbaum et al., 2009). Twenty-four participants (19 male and 5 female) were recruited from the university and local community, and their mean (SD) age, stature, and body mass were 24.2 (4.8) yrs, 174.2 (8.0) cm, and 71.4 (12.8) kg, respectively. All reported being physically active and having no illnesses, injuries, or musculoskeletal disorders within the past year that restricted their daily activities. All participants completed informed consent procedures approved by the Virginia Tech Institutional Review Board.

Following initial measurements, electrode placements, and MVCs, participants performed 10 panel erection trials, which included different types of carrying (C), erecting (E), lifting (L), and moving (M) tasks (Table 1). Each trial was performed under several combinations of panel mass (light vs. heavy, representing unsheathed and sheathed walls) and panel size (small = 1.2 × 2.4 m, medium = 2.4 × 2.4 m, and large = 3.0 × 2.4 m). The set of tasks simulated situations observed in the field (Nussbaum et al., 2009; Kim et al., 2011).

Participants began the trials standing on two force platforms (AMTI OR6-7-1000, Watertown, Massachusetts) with one foot on each. External hand kinetics were monitored using two triaxial load cells (AMTI MC3A-6), placed at self-selected "optimal" locations identified during prior practice trials. EMG, force platform, and load cell signals were collected at 1080 Hz. Whole-body kinematics were recorded using a set of passive reflective markers placed over anatomical landmarks: spinous processes of 7th cervical and 8th thoracic vertebrae and lumbosacral joint, upper and lower arms, lower leg, and heels. Marker data were collected at 120 Hz using a 6-camera system (Vicon 524, Vicon System, Los Angeles, CA). Subsequently, force platform and load cell signals were low-pass filtered with a cut-off frequency of 12 Hz, and marker positions were similarly filtered (cut-off frequency = 9 Hz). EMGs were processed as described in Section 2.6.

Table 1
Summary of simulated panel erection tasks used for model evaluation (see Kim et al., 2011 for further details).

Task	Description	Task	Description
C1	Carrying panel in horizontal orientation	E1KSide	Erecting a panel until it stands vertically with panel initially held at knuckle height and participant standing at panel side
C2	Carrying panel while holding it angled at roughly 45° to the ground	L1G	Lifting a panel horizontally from ground level
E1GTop	Erecting a panel until it stands vertically with panel initially held at ground level and participant standing at the top-plate side of the panel	L1K	Lifting a panel horizontally from an individual's knuckle height level
E1GSide	Erecting a panel until it stands vertically with panel initially held at ground level and participant standing at panel side	L2G	Lifting and titling a panel from 0° to ~45° to the floor at the completion of lifting
E1KTop	Erecting a panel until it stands vertically with panel initially held at knuckle height and participant standing at the top-plate side of the panel	M1	Pushing a vertically placed panel forward along long axis

Model performance was evaluated from data obtained in 1070 trials, by comparing measured and predicted triaxial moments at L5/S1. For each trial, comparison of these moments yielded three performance measures in three rotation planes: coefficient of determination (r^2), absolute root-mean-square (aRMS) difference, and relative root-mean-square (rRMS) difference. The first was chosen to assess overall correspondence, while aRMS was used to indicate absolute differences between predicted and measured moments. rRMS was obtained by normalizing aRMS to within-trial peak moment, and was used to represent the quality of model predictions relative to task demands. Lastly, the cumulative distribution function (CDF) of r^2 was derived to summarize results across trials.

2.8. Statistical analyses

Initially, a multivariate analysis of variance (MANOVA) was conducted to assess the main effects of panel mass, panel size, and erection task on the performance measures (i.e., r^2, aRMS, and rRMS). Where MANOVA showed a significant effect, a repeated ANOVA was used to identify effects on each rotation plane. Note that only main effects were examined, as the experiment did not include factorial combinations and our primary interests were whether model performance might differ between levels of the individual factors. Throughout, a p-value < 0.05 was considered statistically significant, and all summary data are presented as

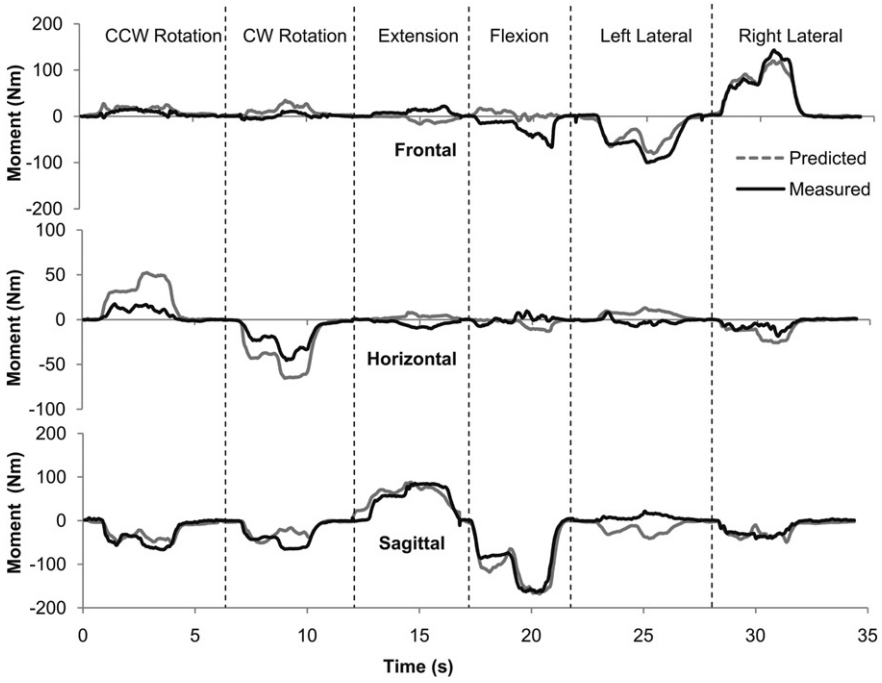

Fig. 1. Representative results from model calibration ($S_E = 40$ N cm^2; $S_F = 110$ N cm^2; $k_1 = 0$; $k_2 = 1.1$; $k_3 = 162$ ms; aRMS = 2.72 N m). Note that all six of the maximal efforts (listed at the top) are concatenated for clarity. Measured external and model-predicted internal lumbosacral moments are shown in each of the three rotation planes (+ = extension, right lateral bending, and CCW rotation for external moments). Predicted (internal) moments are shown with inverted signs, to facilitate comparisons with external moments.

Table 2
Summary of external moments and measures of model performance (across 1070 experimental trials). The 50th and 95th percentile intra-trial moments, overall correspondence (r^2) between measured versus predicted moments, and absolute (aRMS) and relative (rRMS) moment differences are reported in each rotation plane as means (SD).

	Frontal	Horizontal	Sagittal
50%ile moment (N m)	27.3 (12.3)	13.7 (8.7)	109.9 (34.6)
95%ile moment (N m)	116.1 (12.9)	104.0 (8.4)	298.4 (34.6)
r^2	0.54 (0.29)	0.51 (0.31)	0.69 (0.26)
aRMS difference (N m)	6.8 (9.4)	4.8 (5.6)	8.3 (8.0)
rRMS difference (%)	21 (11)	21 (13)	11 (7)

means (SD). All statistical analyses were performed with JMP 7.0 (SAS Institute Inc., Cary, NC).

3. Results

3.1. Model calibration

Calibration procedures yielded muscle stress values (S_F and S_E) of 100.5 (44.4) N/cm^2 for the flexor muscles and 83.2 (39.8) N/cm^2 for the extensor muscles. Parameters describing the EMG-to-force relationship (k_1), muscle passive contribution (k_2), and time lag (k_3) were 0.34 (0.11), 0.9 (0.4), and 162 (54) ms, respectively. Calibrated models yielded a relatively high correspondence between measured and predicted moments in all three planes (representative results shown in Fig. 1). Across all MVC trials aRMS was 3.9 (1.5) N m, and in the passive flexions trials aRMS was 2.4 (2.0) N m.

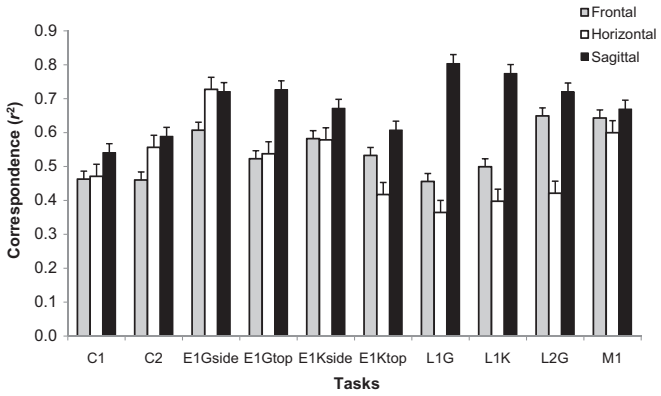

Fig. 3. Summary of measures of overall correspondence (r^2) between measured and model-predicted lumbosacral moments. Mean values are shown for each of the panel erection tasks and for each of the rotation planes. Error bars indicate standard errors.

3.2. Model evaluation

Predictive ability of the EMG-based model was supported by a high correspondence between measured and predicted moments during the panel erection trials (summary in Table 2, representative results in Fig. 2). The CDF of r^2 (correspondence between measured and predicted moments) indicated that 27, 26, and 50% of trials had $r^2 > 0.8$ in the frontal, horizontal and sagittal planes, respectively, and respective proportions of 12, 10, and 28% with $r^2 > 0.9$.

The level of correspondence (r^2) between predicted and measured moments differed across tasks and between the three rotation planes (Fig. 3). In the sagittal plane, horizontal lifting tasks

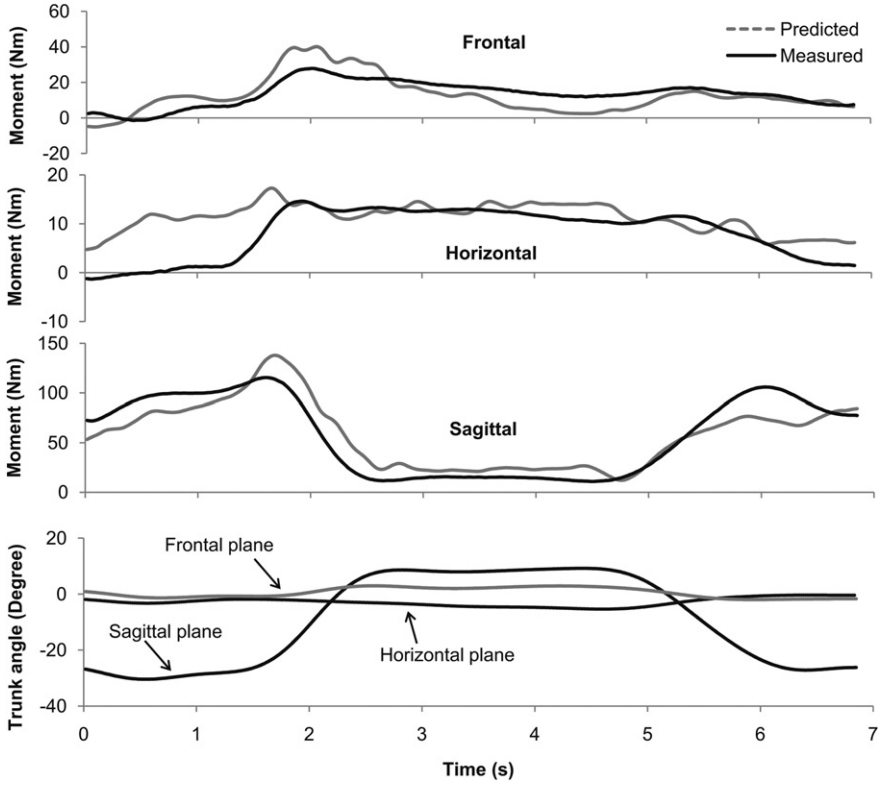

Fig. 2. Representative results from a panel lifting task (L1K: $S_E = 45$ N cm^2; $S_F = 60$ N cm^2; $k_1 = 0$; $k_2 = 1.1$; $k_3 = 108$ ms). Measured and predicted moments at L5/S1 are shown in the top three panels for each rotation plane, with trunk angles shown in the fourth panel (+ = extension, right lateral bending, and CCW rotation for external moments and torso angles). Predicted (internal) moments are shown with inverted signs, to facilitate comparisons with external moments.

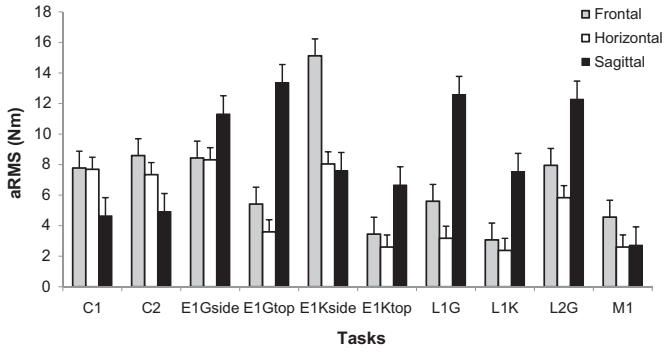

Fig. 4. Summary of measures of absolute RMS (aRMS) differences between measured and model-predicted lumbosacral moments. Mean values are shown for each of the panel erection tasks and for each of the rotation planes. Error bars indicate standard errors.

(L1G and L1K) yielded the highest values [0.80 (0.16) and 0.77 (0.18), respectively], followed by E1Gtop, E1Gside, and L2G which each had comparable r^2 values. Carrying tasks exhibited relatively poorer levels of correspondence [r^2 for C1 = 0.54 (0.29) and for C2 = 0.59 (0.28)]. In the frontal plane, L2G had the best correspondence [0.65 (0.24)], followed by M1, E1Kside, and E1Gside, and L1G yielded the lowest values [0.36 (0.29)]. In the horizontal plane, the highest r^2 value was 0.73 (0.25) for E1Kside, and the lowest was 0.36 (0.29) for L1G. In general, sagittal plane moments had higher r^2 values than either frontal or horizontal plane moments (Table 2).

Typical absolute differences between measured and predicted moments (aRMS) were generally largest in the sagittal plane (Fig. 4). In the frontal plane, aRMS ranged from 2.6 to 8.3 N m across all tasks except for E1Kside [15.1 (15.9) N m]. In the horizontal plane, over half of the tasks resulted had an aRMS difference < 5 N m. In contrast to aRMS, relative differences (rRMS) were smallest in the sagittal plane (Table 2, Fig. 5), and largest in the frontal plane. The largest rRMS differences were found in two lifting tasks (L1G and L2G), while M1 had the lowest rRMS values across the three rotation planes.

Multivariate effects of panel mass, panel size, and panel erection task were each significant (Table 3). Panel erection task also had significant univariate effects on each of the performance measures in all three rotation planes. Panel mass significantly affected aRMS differences in the sagittal plane ($p < 0.01$), with marginally significant effects ($p = 0.05$) in the horizontal and frontal planes. On

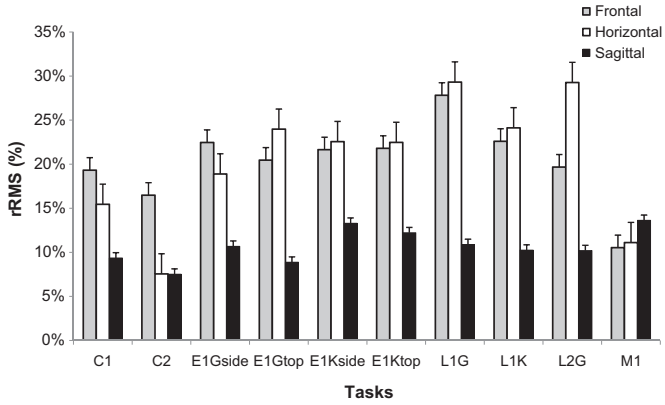

Fig. 5. Summary of measures of relative RMS (rRMS) differences between measured and model-predicted lumbosacral moments. Mean values are shown for each of the panel erection tasks and for each of the rotation planes. Error bars indicate standard errors.

Table 3
Summary of effects (F and p values) of panel size, mass, and erection task on measures of model performance: overall correspondence (r^2), absolute RMS (aRMS), and relative RMS (rRMS). Each measure is based on comparisons of measured vs. predicted moments, and effects are indicated in each rotation plane. Significant effects ($p < 0.05$) are in bold.

		Panel size		Panel mass		Panel erection task	
		$F_{(2,1057)}$	p	$F_{(1,1057)}$	p	$F_{(9,1057)}$	p
MANOVA		2.31	**<0.01**	2.32	**0.015**	21.96	**<0.01**
ANOVA							
r^2	Frontal	0.35	0.71	0.45	0.50	6.17	**<0.01**
	Horizontal	1.86	0.16	0.01	0.97	15.65	**<0.01**
	Sagittal	1.13	0.32	0.26	0.60	11.36	**<0.01**
aRMS	Frontal	2.22	0.11	3.84	**0.050**	25.74	**<0.01**
	Horizontal	1.57	0.21	3.80	**0.052**	33.07	**<0.01**
	Sagittal	1.07	0.36	11.19	**<0.01**	38.67	**<0.01**
rRMS	Frontal	2.24	0.11	2.48	0.12	25.04	**<0.01**
	Horizontal	1.77	0.17	0.01	0.95	29.50	**<0.01**
	Sagittal	4.57	**<0.01**	0.01	0.95	8.31	**<0.01**

average, aRMS differences were 12% larger in the heavy vs. light conditions. Panel size had a significant effect only on rRMS differences in the sagittal plane ($p < 0.01$): large [10.6% (7.0%)] = medium [10.8% (6.8%)] < small [12.2% (8.8%)].

4. Discussion

Given the relatively high prevalence of occupational injuries in residential construction, and the need to refine assessments of physical demands and injury risks associated with a variety of construction tasks, the objective of this study was to extend our original model to predict trunk muscle forces and low back loads during a wide range of panel erection tasks (such tasks are inherently complex and dynamic). This new model incorporated more detailed representations of muscle anatomy and contraction dynamics, and is parameterized using participant-specific values obtained through calibration procedures. With these enhancements, the new model was evaluated in terms of predictive ability, and exhibited reasonable levels of correspondence between measured and predicted lumbosacral moments over the wide range of tasks examined.

Models used to estimate low back loads, particularly during complex and dynamic exertions, should adequately account for intra- and inter-individual variability, muscle cocontraction (synergism and antagonism), and muscle physiological properties. In the present approach, five participant-invariant parameters are determined by collectively considering a set of maximal efforts in each rotation plane along with a passive flexion trial. Note that the calibration procedures included multiple MVC tasks in all three rotation planes, which likely elicited values reasonably close to "true" muscle maxima (McGill, 1991). Muscle stresses estimated here (range: $S_F = 56–145$ N/cm^2; $S_E = 43–123$ N/cm^2) are comparable to ranges reported in earlier studies [$S_F = 40–140$ N/cm^2 and $S_E = 37–105$ N/cm^2 in Nussbaum and Chaffin, 1998; $S = 37–93$ N/cm^2 in Granata and Marras, 1995; $S = 29–108$ N/cm^2 in van Dieën and Kingma, 2005]. The observed range of S_F and S_E values between participants likely indicates that the calibration procedures captured individual differences in muscle stress and PCSA, each of which is difficult to measure directly.

Inter-individual variability in the EMG-to-force relationship (modeled here using k_1) was apparent, in that a linear fit ($k_1 < 0.35$) was obtained for most participants through the iterative estimation procedure yet a nonlinear fit ($k_1 = 1.2$) was identified for three of

them. For the latter, use of a linear fit increased RMS differences between measured and predicted moments by ~23%. Since parameter k_1 was determined using a diverse set of MVCs, its determination implicitly accounted for the contribution of both agonist and antagonist muscles. Brown and McGill (2008) demonstrated that the EMG-to-moment relationship is more linear than nonlinear if antagonist cocontraction is considered. Further, Staudenmann et al. (2007) indicated that high-pass filtering can enhance the contribution of deeper motor units to surface EMG and result in a relative constant power in the high frequency band (150–500 Hz) of EMG signals that could increase the measured activation levels of both agonists and antagonists. Accordingly, the level of cocontraction is likely to be increased, so that the EMG-to-force relationship may become more linear.

Torso flexibility for each participant was modeled by considering intervertebral stiffness and a lumped representation of other passive tissues (using parameter k_2). Relatively large inter-individual variability was found for k_2 [0.9 (0.4)], though these were close to results reported earlier (Nussbaum and Chaffin, 1998). To establish the last model parameter, representing electromechanical delay (k_3), a global time delay (GTD) was introduced. Obtained values [166 (59) ms] were ~30 ms longer than those in earlier work [136.8 (30.9) ms in van Dieën et al., 1991; 132 (27) ms in Nussbaum and Chaffin, 1998], though this discrepancy likely resulted from the current calibration procedures and use of high-pass filtering. Specifically, muscle cocontraction affects the recruitment of different muscle fiber types during a contraction, and hence the onset of measured force output can be altered, which likely changes the time delay (van Dieën et al., 1991). Staudenmann et al. (2007) further suggested that an increased time delay could be explained by an enhanced contribution of deeper motor units induced by high-pass filtering as used here.

Trunk velocity has been demonstrated to have important effects on predicted spinal loads (Granata et al., 1999), and muscle force estimation is affected by contraction type (i.e., concentric and eccentric) and contraction velocity (Bigland and Lippold, 1954; Raschke and Chaffin, 1996). The current model, in contrast to our earlier approach, included an explicit force–velocity relationship (Eq. (2)). This was done to improve predictive ability, as the tasks under investigation were relatively dynamic (i.e., compared to the tasks for the which the earlier model were used). The current work was not intended to rigorously investigate the effects of including a force–velocity relationship on model performance. However, a separate investigation indicated that including the force–velocity relationship significantly and substantially improved predictive ability of the model.

In practice, the panelized construction process includes a variety of tasks as well as different panel masses and sizes. Hence, in the context of our decision support system, model predictions are needed over a wide spectrum of trunk kinematics and muscle activities. Overall, predictive ability of the current model appeared reasonable for the common panel erection tasks and panel design factors (masses and sizes) examined here. Values of r^2 for sagittal plane moments are comparable with those reported in earlier studies (Granata and Marras, 1993; Nussbaum and Chaffin, 1998; Kingma et al., 2001), though the current work examined tasks that were generally more complex and involved a wider variety of kinematics and kinetics. Values for frontal and horizontal plane moments are higher than reported for our earlier model (Nussbaum and Chaffin, 1998), but lower than in some studies (Granata and Marras, 1995; Marras and Granata, 1995). The latter discrepancy may be due to the relatively higher complexity and variety studied here.

Across all experimental trials, the current model yielded somewhat better levels of correspondence (r^2) between measured and predicted lumbosacral moments in the sagittal plane than in other two planes (Table 1). Predictive ability was unaffected by either panel size or mass, but did differ between tasks (Table 2). These differences in predictive ability are, at least in part, explained by trunk dynamics. Depending on both the initial and the final location of a panel and the task type, trunk motions were primarily within one rotation plane (i.e., principle rotation plane), though some conditions involved more substantial motions within this principle plane. Values of r^2 were higher within the principle rotation plane than in the other planes (subordinate rotation planes), perhaps because both external moments and EMG signal-to-noise ratios were larger in the principle rotation plane.

As was the case for overall correspondence between measured and predicted moments (r^2), magnitudes of typical absolute (aRMS) and relative (rRMS) differences were also comparable to those in earlier reports. In previous studies (Cholewicki et al., 1995; Granata and Marras, 1995; Nussbaum and Chaffin, 1998; Gagnon et al., 2001; Kingma et al., 2001), aRMS ranged from 10 to 23 N m in the frontal plane, 9–19 N m in the horizontal plane, and 18–52 N m in the sagittal plane. Somewhat lower respective mean values found here: 6.8, 4.8 and 8.3 N m. In addition, aRMS differences increased significantly with panel mass in all three rotation planes. This effect may have resulted from increases in torso muscle activity with increasing panel mass. As suggested above, there were likely subsequent influences on the magnitude of lumbosacral moments and EMG signal-to-noise ratios. Mean relative (rRMS) differences between measured and predicted moments were 21%, 21% and 11% in the frontal, horizontal and sagittal planes, respectively. The only available comparison data were by Granata and Marras (1995), who reported similar values in the frontal (24%) and sagittal (15%) planes.

As a whole, the comparisons given above suggest that the present model has at least comparable predictive ability to earlier approaches. In terms of absolute predictions errors, however, the current approach appeared somewhat more effective, though it remains to be determined what measures best indicate model performance (e.g., in terms of predicting internal spinal loads). Further, the range of tasks studied here were both more diverse (range of external moments and rotation planes in which these were present) and more complex (external moments at substantial levels in multiple rotation planes simultaneously) than those with which other modeling approaches have been evaluated.

A few limitations in the present work should be acknowledged. First, the current model includes only one motion segment (i.e., L5/S1). Arjmand et al. (2007) showed that estimated muscle forces vary with spinal level if a model considers only a single level, and that muscle forces estimated this way violate equilibrium at remaining spinal levels. Second, consistent with earlier modeling approaches, EMG normalization was done using data obtained in a posture that was not always consistent with postures in which the model was used. Here, maximal EMG values were obtained during MVCs conducted in specified postures (mostly upright), yet the panel erection tasks often involved substantial trunk motions. Since maximal EMG values vary with posture and influence normalized values (Mirka, 1991), this is a likely a non-trivial source of error. Short of an intensive preliminary data collection to obtain maximal EMG values over a range of postures, additional work is needed to address this issue. Third, interpretations based on model predictions in subordinate planes require some caution since these predictions seemed somewhat inferior. Better measurements of trunk kinematics, more precise representations of individual muscular anatomy, and methods to account for inaccessible (deep) muscles may, in the future, help improve model predictive ability.

In summary, a free-dynamic three-dimensional EMG-based biomechanical model has been developed to predict low back loads under various dynamic tasks. Through a calibration

procedure, five model parameters are specified on an individual basis and used to estimate lumbar muscle forces. This model was assessed during a range of common panel erection tasks, and demonstrated a reasonable level of predictive ability. Subsequently, model outputs (e.g., internal spinal loads and muscle forces) will be used as quantitative descriptions of the physical demands and injury risks placed on construction workers during these tasks, which will be incorporated into our ongoing efforts to facilitate proactive design of residential construction using panelized walls. Additional work is underway to investigate effects of panel erection tasks on trunk kinematics and low back loads (e.g., Jia et al., 2009), and the correspondence between trunk kinematics and low back loads will be identified. Further research is still needed, however, to improve predictive ability and to extend the model to multiple spinal levels.

Acknowledgements

The authors thank Dr. Michael J. Agnew for his time and effort during equipment setup, and further extend their appreciation to Leanna M. Horton, Jungyong Lee, and Ranjana Mehta for their help during data collection. This work was supported by Cooperative Agreement Number U19 OH008308 from the Centers for Disease Control and Prevention (CDC). Its contents are solely the responsibility of the authors and do not necessarily represent the official views of CDC.

References

AnyBody, v3.0. Scaling reference: http://www.anybodytech.com/fileadmin/AnyBody/Docs/Tutorials/chap10_Scaling/intro.html.

Arjmand, N., Shirazi-Adl, A., Parnianpour, M., 2007. Trunk biomechanical models based on equilibrium at a single-level violate equilibrium at other levels. Eur. Spine J. 16, 701–709.

Bigland, B., Lippold, O.C.J., 1954. The relation between force, velocity and integrated electrical activity in human muscles. J. Physiol. 123, 214–224.

BLS, 2008a. Nonfatal Occupational Injuries and Illnesses Requiring Days Away From Work in 2008. United States Department of Labor. http://www.bls.gov/iif/oshcfoi1.htm.

BLS, 2008b. Incidence Rates of Nonfatal Occupational Injuries and Illnesses by Industry and Case Types in 2008. United States Department of Labor. http://www.bls.gov/iif/oshcfoi1.htm.

BLS, 2008c. Employment by Occupation, 2008 and Projected 2018. United States Department of Labor. http://www.bls.gov/iif/oshcfoi1.htm.

Bogduk, N., Macintosh, J.E., Pearcy, M.J., 1992. A universal model of the lumbar back muscles in the upright position. Spine 17, 897–913.

Brown, S.H., McGill, S.M., 2008. Co-activation alters the linear versus non-linear impression of the EMG–torque relationship of trunk muscles. J. Biomech. 41, 491–497.

Brown, S.H.M., Brookham, R.L., Dickerson, C.R., 2009. High-pass filtering surface EMG in an attempt to better represent the signals detected at the intramuscular level. Muscle Nerve 43, 6.

Cavanagh, P.R., Komi, P.V., 1979. Electromechanical delay in human skeletal muscle under concentric and eccentric contractions. Eur. J. Appl. Physiol. 42, 159–163.

Chaffin, D.B., Andersson, G., Martin, B.J., 2006. Occupational Biomechanics, fourth ed. Wiley-Interscience, Hoboken, N.J.

Cholewicki, J., McGill, S.M., 1994. EMG assisted optimization: a hybrid approach for estimating muscle forces in an indeterminate biomechanical model. J. Biomech. 27, 1287–1289.

Cholewicki, J., McGill, S.M., 1996. Mechanical stability of the in vivo lumbar spine: implications for injury and chronic low back pain. Clin. Biomech. 11, 1–15.

Cholewicki, J., McGill, S.M., Norman, R.W., 1995. Comparison of muscle forces and joint load from an optimization and EMG assisted lumbar spine model: towards development of a hybrid approach. J. Biomech. 28, 321–331.

Coorevits, P.L.M., Danneels, L.A., Ramon, H., Van Audekercke, R., Cambier, D.C., Vanderstraeten, G.G., 2005. Statistical modelling of fatigue-related electromyographic median frequency characteristics of back and hip muscles during a standardized isometric back extension test. J. Electromyogr. Kinesiol. 15, 444–451.

Danneels, L.A., Cagnie, B.J., Cools, A.M., Vanderstraeten, G.G., Cambier, D.C., Witvrouw, E.E., De Cuyper, H.J., 2001a. Intra-operator and inter-operator reliability of surface electromyography in the clinical evaluation of back muscles. Man. Ther. 6, 145–153.

Danneels, L.A., Vanderstraeten, G.G., Cambier, D.C., Witvrouw, E.E., Stevens, V.K., De Cuyper, H.J., 2001b. A functional subdivision of hip, abdominal, and back muscles during asymmetric lifting. Spine 26, E114–E121.

de Zee, M., Hansen, L., Wong, C., Rasmussen, J., Simonsen, E.B., 2007. A generic detailed rigid-body lumbar spine model. J. Biomech. 40, 1219–1227.

Gagnon, D., Lariviere, C., Loisel, P., 2001. Comparative ability of EMG, optimization, and hybrid modelling approaches to predict trunk muscle forces and lumbar spine loading during dynamic sagittal plane lifting. Clin. Biomech. 16, 359–372.

Gardner-Morse, M.G., Stokes, I.A.F., 2004. Structural behavior of human lumbar spinal motion segments. J. Biomech. 37, 205–212.

Granata, K., Marras, W., 1993. An EMG-assisted model of loads on the lumbar spine during asymmetric trunk extensions. J. Biomech. 26, 1429–1438.

Granata, K.P., Marras, W.S., 1995. An EMG-assisted model of trunk loading during free-dynamic lifting. J. Biomech. 28, 1309–1317.

Granata, K.P., Marras, W.S., Davis, K.G., 1999. Variation in spinal load and trunk dynamics during repeated lifting exertions. Clin. Biomech. 14, 367–375.

Hecker, S., Gambatese, J.A., Weinstein, M., 2004. Designing for Safety and Health in Construction: Proceedings from a Research and Practice Symposium. University of Oregon Press. 318 p.

Hinze, J., Wiegand, F., 1992. Role of designers in construction worker safety. J. Constr. Eng. Manag. 118, 677–684.

Jia, B., Kim, S., Nussbaum, M., 2009. Influence of panelized wall mass and maneuvering tasks on physical demands in residential construction: muscle activity and trunk kinematics. In: Proceedings of the International Ergonomics Association (IEA) Conference, Beijing, China, August 9–14, pp. 103–109.

Keenan, K.G., Valero-Cuevas, F.J., 2008. Epoch length to accurately estimate the amplitude of interference EMG is likely the result of unavoidable amplitude cancellation. Biomed. Signal Process Contr. 3, 154–162.

Kiefer, A., Shirazi-Adl, A., Parnianpour, M., 1998. Synergy of the human spine in neutral postures. Eur. Spine J. 7, 471–479.

Kim, S., Nussbaum, M., Jia, B., 2011. Low back injury risks during construction with prefabricated (panelised) walls: effects of task and design factors. Ergonomics 54, 60–71.

Kingma, I., Baten, C.T.M., Dolan, P., Toussaint, H.M., van Dieën, J.H., de Looze, M.P., Adams, M.A., 2001. Lumbar loading during lifting: a comparative study of three measurement techniques. J. Electromyogr. Kinesiol. 11, 337–345.

Lipscomb, H.J., Dement, J.M., Li, L., Nolan, J., Patterson, D., 2003a. Work-related injuries in residential and drywall carpentry. Appl. Occup. Environ. Hyg. 18, 479.

Lipscomb, H.J., Dement, J.M., Behlman, R., 2003b. Direct costs and patterns of injuries among residential carpenters, 1995–2000. J. Occup. Environ. Med. 45, 875–880.

Marras, W.S., Granata, K.P., 1995. A biomechanical assessment and model of axial twisting in the thoracolumbar spine. Spine 20, 1440–1451.

McGill, S.M., 1991. Electromyographic activity of the abdominal and low back musculature during the generation of isometric and dynamic axial trunk torque: implications for lumbar mechanics. J. Orthop. Res. 9, 91–103.

McGill, S.M., 1992. A myoelectrically based dynamic three-dimensional model to predict loads on lumbar spine tissues during lateral bending. J. Biomech. 25, 395–414.

McGill, S.M., Norman, R.W., 1986. Partitioning of the L4–L5 dynamic moment into disc, ligamentous, and muscular components during lifting. Spine 11, 666–678.

McGill, S.M., Juker, D., Kropf, P., 1996. Appropriately placed surface EMG electrodes reflect deep muscle activity (psoas, quadratus lumborum, abdominal wall) in the lumbar spine. J. Biomech. 29, 1503–1507.

Mirka, G.A., 1991. The quantification of EMG normalization error. Ergonomics 34, 343–352.

Mirka, G.A., Marras, W.S., 1993. A stochastic model of trunk muscle coactivation during trunk bending. Spine 18, 1396–1409.

Mullins, J.P., 2006. Recent employment trends in residential and nonresidential construction. Mon. Labor Rev. 129, 3.

Norman, R.W., Komi, P.V., 1979. Electromechanical delay in skeletal muscle under normal movement conditions. Acta Physiol. Scand. 106, 241–248.

Nussbaum, M.A., Chaffin, D.B., 1996. Evaluation of artificial neural network modelling to predict torso muscle activity. Ergonomics 39, 1430–1444.

Nussbaum, M.A., Chaffin, D.B., 1998. Lumbar muscle force estimation using a subject-invariant 5-parameter EMG-based model. J. Biomech. 31, 667–672.

Nussbaum, M.A., Shewchuk, J.P., Kim, S., Seol, H., Guo, C., 2009. Development of a decision support system for residential construction using panelized walls: approach and preliminary results. Ergonomics 52, 87–103.

O'Brien, W.R., Beliveau, Y., 2002. Industrializing the residential construction site phase three: production system. Prepared for the Department of Housing and Urban Development, Office of Policy Development and Research, Washington, DC 20410.4.

Panjabi, M.M., Krag, M.H., White 3rd, A.A., Southwick, W.O., 1977. Effects of preload on load displacement curves of the lumbar spine. Orthop. Clin. North Am. 8, 181–192.

Potvin, J.R., Brown, S.H., 2004. Less is more: high pass filtering, to remove up to 99% of the surface EMG signal power, improves EMG-based biceps brachii muscle force estimates. J. Electromyogr. Kinesiol. 14, 389–399.

Potvin, J.R., Norman, R.W., McGill, S.M., 1996. Mechanically corrected EMG for the continuous estimation of erector spinae muscle loading during repetitive lifting. Eur. J. Appl. Physiol. Occup. Physiol. 74, 119–132.

Raschke, U., Chaffin, D.B., 1996. Support for a linear length–tension relation of the torso extensor muscles: an investigation of the length and velocity EMG–force relationships. J. Biomech. 29, 1597–1604.

Ross, E.C., Parnianpour, M., Martin, D., 1993. The effects of resistance level on muscle coordination patterns and movement profile during trunk extension. Spine 18, 1829–1838.

Schoonover, T., Bonauto, D., Silverstein, B., Adams, D., Clark, R., 2010. Prioritizing prevention opportunities in the Washington State construction industry, 2003–2007. J. Safety Res. 41, 197–202.
Schulte, P.A., Rinehart, R., Okun, A., Geraci, C.L., Heidel, D.S., 2008. National Prevention through Design (PtD) initiative. J. Safety Res. 39, 115–121.
Staudenmann, D., Potvin, J.R., Kingma, I., Stegeman, D.F., van Dieen, J.H., 2007. Effects of EMG processing on biomechanical models of muscle joint systems: sensitivity of trunk muscle moments, spinal forces, and stability. J. Biomech. 40, 900–909.
Stokes, I.A., Gardner-Morse, M., 1999. Quantitative anatomy of the lumbar musculature. J. Biomech. 32, 311–316.
Stokes, I.A.F., Gardner-Morse, M., 2003. Spinal stiffness increases with axial load: another stabilizing consequence of muscle action. J. Electromyogr. Kinesiol. 13, 397–402.
Theado, E.W., Knapik, G.G., Marras, W.S., 2007. Modification of an EMG-assisted biomechanical model for pushing and pulling. Int. J. Indust. Ergon. 37, 825–831.
Thelen, D.G., Schultz, A.B., Ashton-Miller, J.A., 1995. Co-contraction of lumbar muscles during the development of time-varying triaxial moments. J. Orthop. Res. 13, 390–398.
Thorstensson, A., Carlson, H., 1987. Fibre types in human lumbar back muscles. Acta Physiol. Scand. 131, 195–202.
van Dieën, J.H., 1996. Asymmetry of erector spinae muscle activity in twisted postures and consistency of muscle activation patterns across subjects. Spine 21, 2651–2661.
van Dieën, J.H., 1997. Are recruitment patterns of the trunk musculature compatible with a synergy based on the maximization of endurance? J. Biomech. 30, 1095–1100.
van Dieën, J.H., Kingma, I., 1999. Total trunk muscle force and spinal compression are lower in asymmetric moments as compared to pure extension moments. J. Biomech. 32, 681–687.
van Dieën, J.H., Kingma, I., 2005. Effects of antagonistic co-contraction on differences between electromyography based and optimization based estimates of spinal forces. Ergonomics 48, 411–426.
van Dieën, J.H., Thissen, C.E., van de Ven, A.J., Toussaint, H.M., 1991. The electromechanical delay of the erector spinae muscle: influence of rate of force development, fatigue and electrode location. Eur. J. Appl. Physiol. 63, 216–222.
van Dieën, J.H., Cholewicki, J.P., Radebold, A.M.D., 2003a. Trunk muscle recruitment patterns in patients with low back pain enhance the stability of the lumbar spine. Spine 28, 834–841.
van Dieën, J.H., Kingma, I., van der Bug, P., 2003b. Evidence for a role of antagonistic cocontraction in controlling trunk stiffness during lifting. J. Biomech. 36, 1829–1836.
Viitasalo, J.H., Komi, P.V., 1975. Signal characteristics of EMG with special reference to reproducibility of measurements. Acta Physiol. Scand. 93, 531–539.
Vink, P., van der Velde, E.A., Verbout, A.J., 1987. A functional subdivision of the lumbar extensor musculature. Recruitment patterns and force–RA–EMG relationships under isometric conditions. Electromyogr. Clin. Neurophysiol. 27, 517–525.
Vink, P., Daanen, H.A.M., Verbout, A., 1989. Specificity of surface-EMG on the intrinsic lumbar back muscles. Hum. Mov. Sci. 8.
Vos, E.J., Mullender, M.G., van Ingen Schenau, G.J., 1990. Electromechanical delay in the vastus lateralis muscle during dynamic isometric contractions. Eur. J. Appl. Physiol. Occup. Physiol. 60, 467–471.
Wakefield, R., O'Brien, M., Beliveau, Y., 2001. Industrializing the Residential Construction Site Phase Two: Information Integration. Office of Policy Development and Research.
Waters, T.R., Putz-anderson, V., Garg, A., Fine, L.J., 1994. Applications manual for the revised NIOSH lifting equation. DHHS (NIOSH) Publication 94-110.